

Eclipsing binaries in the open cluster NGC 2243 - II. Absolute properties of NV CMa *

J. K a l u z n y¹, W. P y c h¹, S. M. Rucinski²
and I. B. T h o m p s o n³

¹Nicolaus Copernicus Astronomical Center, ul. Bartycka 18, 00-716 Warsaw,
Poland

e-mail: (jka,pych@camk.edu.pl)

²David Dunlap Observatory, Department of Astronomy and Astrophysics,
University of Toronto, P.O. Box 360, Richmond Hill, ON L4C 4Y6, Canada

e-mail: (rucinski@astro.utoronto.ca)

³Carnegie Institution of Washington, 813 Santa Barbara Street, Pasadena, CA
91101, USA

e-mail: (ian@ociw.edu)

ABSTRACT

We present echelle spectroscopic data for five eclipsing binary stars and two giant stars in the field of the open cluster NGC 2243. The average cluster velocity is determined to be $+60.4 \pm 0.6 \text{ km s}^{-1}$. Four of the eclipsing binaries are very likely members of the cluster based on their observed radial velocities. The absolute parameters of cluster member NV CMa are determined by analysing photometric and radial velocity data. We obtain $1.089 \pm 0.010 M_{\odot}$ and $1.221 \pm 0.031 R_{\odot}$ for the primary, and $1.069 \pm 0.010 M_{\odot}$ and $1.178 \pm 0.037 R_{\odot}$ for the secondary. Both components of the binary are located on the Main Sequence, about 1 mag. below the turn-off point on the cluster color-magnitude diagram. Using model age-luminosity and age-radius relations we obtain $4.35 \pm 0.25 \text{ Gyr}$ for the age of NV CMa. The derived age is, however, very sensitive to the adopted metallicity of the cluster. We demonstrate that a meaningful determination of the ages of objects like NV CMa based on evolutionary models is possible only if their metallicity is known with a relative accuracy of a few percent. The distance moduli calculated for the components of NV CMa agree closely with each other, and imply an apparent distance modulus of the cluster of $(m - M)_{\text{V}} = 13.25 \pm 0.08$.

Stars: binaries: eclipsing, binaries – stars: individual: NV CMa – open clusters and associations: individual: NGC 2243

1 Introduction

The field of the intermediate-age open cluster NGC 2243 contains 5 known detached eclipsing binaries. Four of these are likely cluster members based on their photometric properties (Kaluzny et al. 2006; hereafter KKTS). The components of these systems should have the same age, metallicity and heliocentric distance and the determination of their absolute parameters can provide an interesting test of evolutionary models of low mass stars. Moreover, through the use of the surface brightness method, one may obtain a direct measure of the cluster distance.

This paper is focused on the determination of the absolute properties of NV CMa, an eclipsing binary located in the central area of NGC 2243. In addition we use spectroscopic observations to check on the membership status of 4 other binaries in the cluster field.

*This paper includes data obtained with the 6.5-meter Magellan Telescopes located at Las Campanas Observatory, Chile.

2 Spectroscopic Observations and Reductions

Spectroscopic observations of NGC 2243 stars were carried out with the MIKE echelle spectrograph (Bernstein et al. 2003) on the Magellan II (Clay) telescope of the Las Campanas Observatory. The data were collected during observing runs in 2004 October and 2005 September. For this analysis we use data obtained with the blue channel of MIKE covering the range from 400 to 500 nm with a resolving power of $\lambda/\Delta\lambda \approx 38,000$. All of the observations were obtained with a 0.7×5.0 arcsec slit and with 2×2 pixel binning. At 4380 Å the resolution was ~ 2.7 pixels at a scale of 0.043 Å/pixel. The seeing ranged from 0.7 to 1.1 arcsec. The spectra were first processed using a pipeline developed by Dan Kelson following the formalism of Kelson (2003, 2006) and then analysed further using standard tasks in the IRAF/Echelle package[†]. Each of the final individual spectra consisted of two 600 s exposures interlaced with an exposure of a thorium-argon lamp. We obtained 12 spectra of NV CMa. The average signal-to-noise ratios range from 25 at shorter wavelengths to 50 at longer wavelengths. In addition to observations of NV CMa we also obtained single spectra of the eclipsing binaries V4=NS CMa, V5=NX CMa, V7 and V9 (names of variables as in KKTS), and for the red giants H3110 and H4115 (Hawarden 1975) located in the central part of the cluster field.

2.1 Spectroscopic Orbit of NV CMa

Radial velocities of the components of NV CMa were measured by cross-correlation with the FXCOR task in IRAF, using observations of HD 33256 as a template. According to Nordstrom et al. (2004), HD 33256 has $V_{rad} = 10.1 \pm 0.2 \text{ km s}^{-1}$ and a projected rotational velocity $V \sin i = 10 \text{ km s}^{-1}$. With $B - V = 0.45$ and $[\text{Fe}/\text{H}] = -0.5$, it provides a good match for the color index and metallicity of the binary. The template was observed with the same instrumental configuration as the variable. The correlation peaks were measured to have a FWHM of about 70 km s^{-1} . All spectra showed the peaks to be separated by more than 1.4 FWHM, and the peaks were measured simultaneously with the FXCOR package. The correlation was measured only from the metal lines, excluding the H β , H γ , and H δ hydrogen lines. Our velocity measurements for NV CMa are listed in Table 1 and are shown in Fig. 1. A Keplerian orbit was fitted to the observations by fixing the period and epoch based on the precise ephemeris established by KKTS:

$$MinI = HJD\ 2448663.70748(5) + 1.18851590(2) \quad (1)$$

We assumed a circular orbit based on the photometric data. This assumption is further supported by the relatively short orbital period of the variable compared to the cluster age of about 3.8 Gyr (Anthony-Twarog, Atwell & Twarog 2005). For an age of 3.8 Gyr all NGC 2243 binaries with periods shorter than a few days are expected to have circularized orbits (Mathieu 2005). The adjustable parameters in the orbital solution were the velocity semi-amplitudes (K_1 and K_2) and the systemic velocity (γ). The fit was performed using the GAUSSFIT task within IRAF/STSDAS. The derived parameters of the spectroscopic orbit are listed in Table 2[‡]. The systemic velocity of NV CMa agrees within the

[†]IRAF is distributed by the National Optical Astronomy Observatories, which are operated by the Association of Universities for Research in Astronomy, Inc., under cooperative agreement with the NSF.

[‡]Through this paper we adopt the following values of constants: $R_{\odot} = 6.95508E5 \text{ km}$, $M_{\odot} = 1.9891E30 \text{ kg}$, $G = 6.67259E - 11 \text{ m}^3\text{kg}^{-1}\text{s}^{-2}$.

Table 1: Radial velocities of NV CMa and residuals from the adopted spectroscopic orbit

Phase	HJD-2453000	RV_1	σ_{RV1}	RV_2	σ_{RV2}	$(O - C)_A$	$(O - C)_B$
0.2634	724.7208	-67.20	2.77	192.23	2.69	-0.81	0.12
0.3178	636.8353	-56.61	1.50	182.27	1.51	-1.25	1.40
0.3375	636.8587	-45.65	1.51	173.65	2.04	2.26	0.36
0.3557	636.8803	-40.76	1.31	161.51	1.80	-1.23	-3.24
0.4344	282.7961	12.29	1.26	114.13	1.18	2.09	0.00
0.5930	281.7961	134.08	1.06	-11.81	1.10	1.47	-1.32
0.6100	281.8163	143.47	1.02	-22.17	1.10	-0.17	-0.45
0.6259	281.8353	152.98	1.18	-31.36	1.14	-0.13	0.00
0.6422	281.8546	160.28	1.22	-40.58	1.26	-1.59	-0.30
0.6582	281.8736	170.66	1.31	-49.45	1.39	1.21	-1.45
0.8310	633.8797	173.11	1.26	-51.55	1.55	-0.85	1.03
0.8401	633.8905	170.83	1.35	-46.98	1.47	0.63	1.77

Table 2: Orbital parameters of NV CMa.

Parameter	Value
P (days)	1.18851590(fixed)
T_0 (HJD-244 0000)	8663.70748(fixed)
γ ($km\ s^{-1}$)	61.70 ± 0.30
e	0(fixed)
K_1 ($km\ s^{-1}$)	128.55 ± 0.52
K_2 ($km\ s^{-1}$)	130.87 ± 0.55
Derived quantities:	
$A \sin i$ (R_\odot)	6.096 ± 0.018
$M_1 \sin^3 i$ (M_\odot)	1.084 ± 0.010
$M_2 \sin^3 i$ (M_\odot)	1.065 ± 0.010
Other quantities:	
σ_1 ($km\ s^{-1}$)	1.37
σ_2 ($km\ s^{-1}$)	1.37

measurement errors with the radial velocity of the cluster as estimated in the next subsection.

2.2 Analysis of Broadening Functions

We have analysed the spectra of NV CMa using code based on the broadening function (BF) formalism (Rucinski 2002). The BF analysis lets us study the effects of the spectral line broadening and orbital splitting even for relatively complicated profiles of spectral lines. This macroscopic velocity information is obtained regardless of the parameters of the photosphere such as the temperature, pressure etc. It retains strict linearity in reproduction of the individual contributions to the broadening profile, i.e. the individual luminosities of components can be simply estimated from the strengths of the respective peaks in the broadening profile.

In the case of detached binary systems the dominating effect on the observed broadening of the spectral lines comes from the rotation of the components induced by the orbital motion. If we make the approximation of rigid rotation of perfectly spherical stars we can integrate the light over the visible hemispheres

analytically. The resulting theoretical rotational BF has a shape described by:

$$BF_{rot}(v) = A[(1-\beta)\sqrt{1-a^2} + \frac{\pi}{4}\beta(1-a^2)] + C \quad (2)$$

$$a = \frac{v - v_{rad}}{v_{rot} \sin i}$$

where A is a normalization constant, β is the linear limb darkening coefficient, C is the continuum level, v_{rad} is the radial velocity of the center of mass of the star, v_{rot} is the linear velocity on the equator of the rotating star, and i is the inclination angle between the axis of rotation and the direction to the observer.

We have extracted BFs from all of the spectra of NV CMa and have conducted nonlinear least squares fitting of the model profile to the observed BFs to measure the radial and projected rotational velocities of the components of NV CMa. In both steps of the calculation we have used our programs based on procedures from the GNU Scientific Library.

As it will be shown in Section 3, the components of NV CMa are almost spherical and there are no signatures of spot activity. Our model profile is then the sum of two theoretical rotational BFs convolved with a Gaussian with a standard deviation of 15 km s^{-1} . The Gaussian represents effects of the instrumental resolution and is a part of the BF method in which modest smoothing (adjusted to the width of the spectrograph slit image) is applied to the BFs. We used the spectra in the wavelength range from 400 nm to 495 nm . This range roughly corresponds to the B passband in the UBV photometric system. Since the shape of the rotational BF only weakly depends on the limb darkening coefficient, we have adopted a constant $\beta=0.63$ as derived from the $(B-V, \beta)$ relation of van Hamme (1993). The four parameters A , C , v_{rad} , and $v_{rot} \sin i$ were simultaneously adjusted in the fitting procedure. Figure 2 presents an example of fitting the model to the BF calculated for a spectrum taken at orbital phase 0.61. A linear least squares fit to the measured radial velocities gives the following orbital solution: $\gamma = 61.47 \pm 0.14 \text{ km s}^{-1}$, $K_1 = 130.93 \pm 0.59 \text{ km s}^{-1}$, $K_2 = 128.62 \pm 0.42 \text{ km s}^{-1}$, which lies well within formal errors from the result obtained using the cross-correlation analysis. The RMS error of the fit is 0.93 km s^{-1} for both components. We measure the projected rotational velocities to be $V_1 \sin i = 51.7 \pm 1.4 \text{ km s}^{-1}$ and $V_2 \sin i = 52.4 \pm 2.5 \text{ km s}^{-1}$. Note that these rotational velocities are very close to those expected if the components are in synchronous rotation in a circular orbit, adopting the period from Table 2 and the stellar radii from Table 1 ($V_1 \sin i = 52.0 \pm 1.3 \text{ km s}^{-1}$ and $V_2 \sin i = 50.1 \pm 1.6 \text{ km s}^{-1}$). [SMR: Strictly speaking, we should subtract quadratically the Gaussian smoothing of $\sigma = 15 \text{ km/s}$. Then one gets 49.5 and 50.2 km/s, in almost perfect agreement with the expectations.]

The integral of a BF profile is proportional to the total flux from a star. Since the absolute measurement of this flux requires a perfect match between the template and object spectra we did not attempt to conduct such an analysis. However, given that the effective temperatures of the components of NV CMa are very similar, the integrals of the BF profiles are proportional to the monochromatic luminosities of the two components. An analytical integration of the profiles leads to the conclusion that the ratio of the luminosities of stars with identical spectral types is proportional to the ratio of the products $A \cdot v_{rot} \sin i$ for each of the system components. From a total of 11 spectra with well defined BF profiles we obtained $L_{1B}/L_{2B} = 1.087 \pm 0.011$ ($rms = 0.034$), in good agreement with the values measured from the photometric observations (see Section 3).

Table 3: Radial velocities of stars from the field of NGC 2243

Name	HJD-2450000	RV ₁	RV ₂	member?
H3110	3281.9127	59.4(1.0)		yes
H4115	3281.9285	60.1(1.1)		yes
V4	3635.9006	117.5(2.4)	285.9(9.6)	no
V5	3638.8430	23.50(0.58)	94.61(0.56)	yes
V7	3638.8217	96.88(0.80)	22.8(5.3)	yes
V9	3638.8711	65.45(0.68)		yes

2.3 Velocities of other objects

Table 2 lists the radial velocities derived for two red giants and four other eclipsing binaries from the cluster field. The velocities of H3110 and H4115 are close to the velocities of two other cluster red giants observed by Gratton (1982) who measured $V_{rad}=+62 \text{ km s}^{-1}$ and $V_{rad}=+60 \text{ km s}^{-1}$ for H4110 and H4209, respectively. Based on these four stars we estimate the radial velocity of the cluster to be $V_{rad}=+60.4 \pm 0.6 \text{ km s}^{-1}$.

Two velocity peaks are seen in the cross-correlation functions of V4, V5, and V7. The mean velocity for the two peaks for V4 is 210.7 km s^{-1} , well above the cluster velocity. We conclude that V4 is a field binary star not related to the cluster. In the case of V5, two peaks of very similar shape and height are seen in the cross-correlation function. The average velocity of the two components is 59.1 km s^{-1} . V5 is a very likely member of the cluster with a mass ratio close to unity. Three peaks show up in the cross-correlation function obtained for V7, one at 22.8 km s^{-1} , one at 96.5 km s^{-1} and a wing to that component at 136.8 km s^{-1} . The mean of first two is 59.6 km s^{-1} , very similar to the cluster average velocity. It is possible that the component with highest velocity is caused by contaminating light from the close visual companion of V7 whose light leaked through the slit during observations (see finding chart in KKTS). For V9 only one strong peak was detected in the cross-correlation function at a velocity of 65.4 km s^{-1} , consistent with cluster membership. It is possible that this binary was observed close to conjunction, and further observations are needed to see if the secondary component can be detected in the cross-correlation function. In conclusion, variables V5, V7 and V9 are likely members of NGC 2243. These three binaries are promising targets for detailed observations aimed at the determination of the parameters of their components.

3 Light Curve Solution of NV CMa

We have analysed the BV light curves of NV CMa obtained by KKTS using the Wilson-Deviney model (Wilson & Deviney 1971) as implemented in the light-curve analysis program MINGA[§] (Plewa 1988). The mass-ratio of the binary was fixed at the spectroscopic value of $m_2/m_1 = 0.9825 \pm 0.0018$. The gravity darkening exponents and bolometric albedos were fixed at 0.32 and 0.5, respectively. The linear darkening coefficients were adopted for the B and V filters from van Hamme (1993) for an assumed metallicity of $[\text{Fe}/\text{H}] = -0.49$ (Gratton & Contarini 1994; Friel et al. 2002). An interpolation routine in the PHOEBE package (Prša & Zwitter 2005) was used to get values corresponding to the adopted effective temperatures of the two components. The light curves

[§]MINGA is available at <http://ftp.camk.edu.pl/camk/tomek/Minga/>

used in the analysis are shown in Fig. 3. They contain 121 points in the B band and 446 points in the V band. Outside of the eclipses, we used normal points formed by averaging 3 to 7 individual observations. There is no evidence for totality in any of the eclipses. The primary and secondary eclipses have very similar depths, implying similar surface brightness and in turn similar effective temperatures for the two components. The light curve is symmetric, indicating that its shape is not noticeably affected by spot activity.

The average color index near quadrature is $\langle B - V \rangle_{max} = 0.439 \pm 0.020$. The quoted uncertainty includes an external error arising from the photometric calibration. Adopting $E(B - V) = 0.055 \pm 0.004$ (Anthony-Twarog et al. 2005) we obtain an unreddened color index at maximum light of $(B - V)_0 = 0.384$. Using the empirical calibration of Ramírez & Meléndez (2005) we get an effective temperature of the primary component of NV CMa of $T_1 = 6522 \pm 129$ K. The uncertainty includes the formal uncertainty in the temperature calibration as well as the uncertainty of the color index. As it is shown below, the effective temperatures of the components do not differ by more than about 30 K and the color index at maximum light can be safely adopted as the color index of the primary component.

The following parameters were adjustable in the light curve solution: the orbital inclination i , the non-dimensional potentials Ω_1 and Ω_2 , the effective temperature of the secondary T_2 , and the relative luminosity of the primary $L_1(V; B)$. For a fixed value of the mass ratio q the potentials Ω_1 and Ω_2 directly determine the relative radii of the components r_1 and r_2 . In the following discussion we list "equal volume" mean radii of the components. Our finally adopted solution (see below) implies that for both components of NV CMa the difference between "polar" and "point" radii amounts to about 2%[¶]. An unconstrained light curve solution obtained with MINGA is listed in Table 4. It is worth noting at this point that the errors returned by MINGA take into account correlations between all fitted parameters. One should note the rather large uncertainties of the derived relative radii and luminosities. This is not an unexpected result given the partial eclipses (Irwin 1962). An additional complication is that the effective temperatures of the components of NV CMa are very similar.

The accuracy of the fit can be significantly improved by using information about the light ratio of the two components derived from the spectroscopic data. A grid of solutions was calculated with a fixed value of Ω_1 (this is equivalent to fixing the value of the radius $\langle r_1 \rangle$). The result is presented graphically in Fig. 3 which shows the calculated values of L_{1B}/L_{2B} and $\langle r_2 \rangle$ as a function of the assumed value of $\langle r_1 \rangle$. There is a strong anti-correlation between the calculated value of $\langle r_2 \rangle$ and the assumed value of $\langle r_1 \rangle$. The solutions fulfill the condition $L_{1B}/L_{2B} = 1.087 \pm 0.011$ only for a very narrow range of radii, from $\langle r_1 \rangle = 0.2001$ to $\langle r_1 \rangle = 0.2014$. However, the uncertainty in $\langle r_1 \rangle$ obtained this way is severely underestimated. To get a realistic estimate of the errors in the fitted parameters one has to take into account correlations between them. To attain that goal we derived solutions for 3 fixed values of L_{1B}/L_{2B} spanning the range 1.087 ± 0.011 . The adjustable parameters were i , Ω_1 , Ω_2 , T_2 and (L_{1V}/L_{2V}) . The final light curve solution along with the uncertainties of all fitted parameters is listed in Table 5. Figure 5 shows the residuals corresponding to this solution.

[¶]The "polar radii" is a radius toward the stellar pole while "point radii" is the radius toward the Lagrangian point L1 of the binary orbit.

Table 4: An unconstrained light curve solution

Parameter	Value
i (deg)	87.08 ± 0.95
Ω_1	5.959 ± 0.332
Ω_2	6.141 ± 0.392
T_1 (K)	6522 (fixed)
T_2 (K)	6512 ± 123
(L_{1V}/L_{2V})	1.110 ± 0.017
(L_{1B}/L_{2B})	1.112 ± 0.024
$\langle r_1 \rangle$	0.203 ± 0.013
$\langle r_1 \rangle$	0.193 ± 0.014
rms (V) (mag)	0.008
rms (B) (mag)	0.006

Table 5: Constrained light curve solution with $(L_{1B}/L_{2B}) = 1.087 \pm 0.011$

Parameter	Value
i (deg)	87.09 ± 0.66
Ω_1	6.010 ± 0.136
Ω_2	6.128 ± 0.155
T_1 (K)	6522 (fixed)
T_2 (K)	6506 ± 75
(L_{1V}/L_{2V})	1.088 ± 0.024
$\langle r_1 \rangle$	0.200 ± 0.005
$\langle r_2 \rangle$	0.193 ± 0.006
rms (B) (mag)	0.008
rms (V) (mag)	0.006

4 Absolute properties

The absolute parameters of NV CMa obtained from our spectroscopic and photometric analysis are given in Table 6. The errors in the temperatures include all sources of uncertainties. The absolute visual magnitudes M_V were calculated using bolometric corrections derived from relations presented by VandenBerg & Clem (2003). The observed visual magnitudes derived from the light curve solutions are $V_1 = 17.107 \pm 0.023$ and $V_2 = 17.199 \pm 0.024$, where the uncertainties include the errors of the photometric zero point. For the B band we obtain $B_1 = 17.549 \pm 0.021$ and $B_2 = 17.640 \pm 0.021$. Figure 6 shows the location of the individual components of NV CMa on a color-magnitude diagram at the turnoff region of NGC 2243. Note that NV CMa lies on the binary sequence in this cluster (Bonifazi et al. 1990) while the individual components lie on the sequence of single stars, further confirmation of the cluster membership of NV CMa. Using these values for the observed and absolute visual magnitudes one obtains an apparent distance modulus $(m - M)_V = 13.25 \pm 0.10$ and $(m - M)_V = 13.25 \pm 0.15$ for the primary and the secondary components of the binary, respectively, with an average value of $(m - M)_V = 13.25 \pm 0.08$. This value is in good agreement with recent determinations of $(m - M)_V = 13.15 \pm 0.1$ obtained from the isochrone fitting method by both Anthony-Twarog et al. (2005; they adopted $[\text{Fe}/\text{H}] = -0.57$) and VandenBerg et al. (2006; they adopted $[\text{Fe}/\text{H}] = -0.61$).

4.1 The age

It is possible to estimate ages of the components of the binary by using theoretical age-luminosity relations. It is worth noting that age-luminosity relations based on stellar models are unaffected by uncertainties associated with model isochrones relating T_{eff} and L_{bol} to color index and absolute magnitude in a selected band. In particular, they are unaffected by the way in which models treat sub-photospheric convection in low mass stars. In Fig. 7 we show age versus luminosity relations based on evolutionary tracks recently published by VandenBerg et al. (2006). The tracks were derived from a set of isochrones calculated with the program *vriso* distributed with the model grids. Models for $[\text{Fe}/\text{H}] = -0.525$ (see the following section) and $[\alpha/\text{Fe}] = 0.3$ were used. Horizontal lines in Fig. 7 mark $L \pm \sigma_L$ ranges for a given component. The intersections of age-luminosity relations with lines marking 1σ limits of the luminosities give limits on the age for a given mass. The 1σ age limits are $4.00 < t_1 < 5.8$ Gyr and $4.1 < t_2 < 6.3$ Gyr for the primary and secondary components of NV CMa, respectively. The large ranges result mainly from the fact that both components are still in a relatively slow phase of their evolution: as can be seen in Fig. 6 they are located about 1 mag. below the turn-off point on the cluster color-magnitude diagram. One may also note from Fig. 7 that the errors of the luminosities and masses contribute an equal 0.6 Gyr to the total uncertainty in the estimated ages.

Figure 8 shows the time dependence of the radius, also a sensitive diagnostic for the age, using the same set of evolutionary models. As before, the solid lines correspond to evolutionary tracks for the masses of components of NV CMa. The measured radii are indicated by the horizontal lines spanning the range $\pm 1\sigma$.

From Fig. 8 we derive 1σ limits on the ages of the components of NV CMa of $3.2 < t_1 < 4.6$ Gyr and $3.2 < t_2 < 4.9$ Gyr. These limits are consistent with those derived from the age-luminosity relations. The age-radius relations suggest slightly lower ages in comparison with the age-luminosity relation for both components. The overlap of the age estimates implies an age for NV CMa of approximately 4.1 to 4.6 Gyr.

4.2 Metallicity

The age estimates presented in the previous section suffer from a potential systematic error arising from the adopted metallicity of NV CMa. There are three modern determinations of the cluster metallicity. Gratton & Contarini (1994) obtained high resolution spectra of two cluster giants and derived $[\text{Fe}/\text{H}] = -0.48 \pm 0.15$. Friel et al. (2002) used medium resolution spectra of 9 stars to derive $[\text{Fe}/\text{H}] = -0.49 \pm 0.05$. Finally, Anthony-Twarog et al. (2005) employed *uvbyCaH β* photometry to obtain $[\text{Fe}/\text{H}] = -0.57 \pm 0.03$. The weighted average of these three determinations gives $[\text{Fe}/\text{H}] = -0.547 \pm 0.025$. This value is very close to $[\text{Fe}/\text{H}] = -0.525$ for which we extracted the model relations used above. However, the estimated age of NV CMa is very sensitive to the adopted metallicity. For example, using models for $[\text{Fe}/\text{H}] = -0.397$ and $[\text{Fe}/\text{H}] = -0.606$ we obtain ages $t = 5.425 \pm 0.025$ Gyr and $t = 3.85 \pm 0.45$ Gyr, respectively, where the very small formal errors just indicate the marginal overlap between the age ranges obtained from age-luminosity and age-radius relations. In summary, for the masses and ages relevant to the present discussion, the metallicity of the analysed stars has to be known with a relative accuracy of a few percent to

Table 6: Absolute parameters of NV CMa

Parameter	Value
A (R_{\odot})	6.104 ± 0.018
M_1 (M_{\odot})	1.089 ± 0.010
M_2 (M_{\odot})	1.069 ± 0.010
R_1 (R_{\odot})	1.221 ± 0.031
R_2 (R_{\odot})	1.178 ± 0.037
T_1 (K)	6522 ± 129
T_2 (K)	6506 ± 149
$Lbol_1$ (L_{\odot})	2.42 ± 0.23
$Lbol_2$ (L_{\odot})	2.23 ± 0.25
M_{V1} (<i>mag</i>)	3.86 ± 0.10
M_{V2} (<i>mag</i>)	3.95 ± 0.15

allow meaningful comparison of observational data with the models. This is illustrated in Fig. 9 which shows age-luminosity and age-radius relations for a star with $m = 1.089m_{\odot}$ and for 3 values of metallicity. The plotted relations are based on models by VandenBerg et al. (2006) for $[\alpha/\text{Fe}] = +0.3$. At a given age the separation between relations for close, but different, metallicities exceeds the uncertainties of the luminosities and radii of components of NV CMa obtained in our analysis presented above.

5 Discussion and summary

The analysis of photometric and spectroscopic observations of the eclipsing binary NV CMA has allowed us to determine the orbital parameters and physical properties of the component stars. Our determinations have formal uncertainties of 1% in the masses and 3% in radii. Uncomfortably large uncertainties in the radii result from the degeneracy of the light curve solution for this partially eclipsing system. Comparison with model tracks for $[\text{Fe}/\text{H}] = -0.525$ give an age of 4.1 to 4.6 Gyr for the binary and consequently for the cluster. This determination suffers from a substantial systematic error related to the uncertain metallicity of the cluster. For the relevant range of stellar masses and ages an uncertainty in the metallicity of 0.1 dex leads to an uncertainty in the estimated age of about 0.8 Gyr.

There is still room for obtaining a better determination of the parameters of NV CMA, including its age. First of all, it is straightforward to derive masses of the components with an accuracy of 0.5% or even better. We used 12 spectra only and additional radial velocity data obtained near quadrature will lead to an improvement in the estimates of the masses of the components. It is also possible to obtain better light curves than these used in the present analysis; an improvement is possible in both the quality and the phase coverage. In particular, our photometry for the B band had poor coverage inside the primary eclipse. Improved light curves would better constrain the parameters of the components obtained in the light curve solution. And last, but not least, the age determination of NV CMA and of other cluster binaries would benefit enormously from accurate metallicity determinations, preferably based on high resolution spectroscopy of an extended sample of cluster member stars.

The analysis of single spectra obtained for four other eclipsing binaries in the cluster field indicates that three of them are radial velocity members of NGC 2243. The fourth star is definitely a non-member. Further observations

of member binaries would allow a better constraint on the cluster age as well as a test of evolutionary models of low-mass stars with $[\text{Fe}/\text{H}] \approx -0.5$.

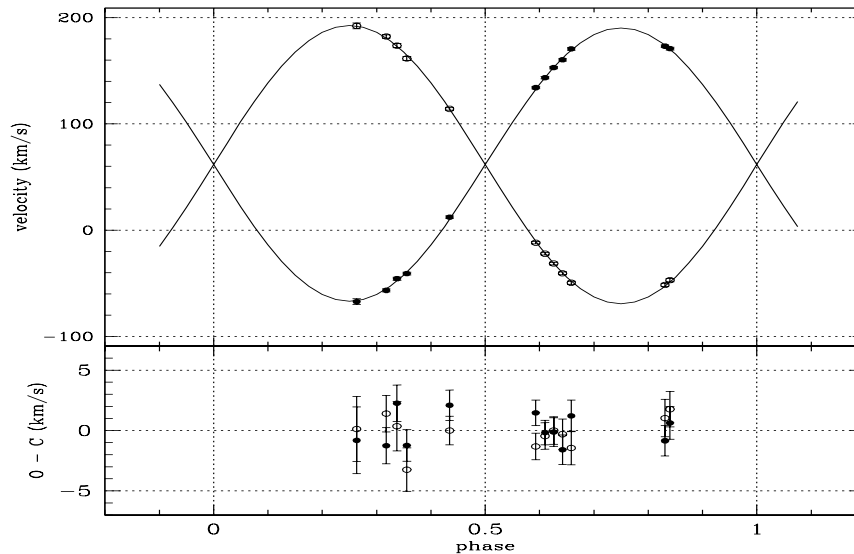


Fig. 1. Spectroscopic observations and adopted orbit for NV CMa.

Acknowledgements. JK and WP were supported by the grant 1 P03D 001 28 from the Ministry of Science and Information Society Technologies, Poland. Research of SMR is supported by a grant from the Natural Sciences and Engineering Council of Canada while IBT is supported by NSF grant AST-0507325. We thank Alexis Brandeker who obtained one of the spectra of NV CMa used here. It is also a pleasure to thank Tomek Plewa for enlightening hints on MINGA usage.

REFERENCES

- Anthony-Twarog, B. J., Atwell, J., Twarog, B. A. 2005, *Astron. J.*, **129**, 872.
 Bergbusch, P. A., Vandenberg, D. A., Infante, L 1991, *Astron. J.*, **101**, 2102.
 Bernstein, R., Sheiman, S. A., Gunnels, S. M., Mochnacki, S., Athey, A. E. 2003, *Instrument Design and Performance for Optical/Infrared Ground-based Telescopes. Edited by Iye, Masanori; Moorwood, Alan F. M. Proceedings of the SPIE*, **4841**, 1694.
 Bonifazi, F., Fusi Pecci, F., Romeo, G., & Tosi, M. 1990, *MNRAS*, **245**, 15.
 Friel, E. D., Janes, K. A., Tavaréz, M., Scott, J., Hong, L., & Miller, N. 2002, *Astron. J.*, **124**, 2693.
 Gratton, R. G. 1982, *Astrophys. J.*, **257**, 640.
 Gratton, R. G., & Contarini, G. 1994, *Astron. Astrophys.*, **283**, 911.
 Hawarden, T. G. 1975, *MNRAS*, **173**, 801.
 Irwin, J. B 1962, in *Astronomical Techniques*, ed. W. A. Hiltner, The University of Chicago Press, , 584.
 Kaluzny, J., Krzeminski, W., & Mazur, B. 1996, *Astron. Astrophys. Suppl. Ser.*, **118**, 303 (KKM).
 Kaluzny, J., Krzeminski, W., Thomspon, I. B., & Stachowski, G. 2006, *Acta Astron.*, **56**, 51 (KKTS).
 Kelson, D. D. 2003, *P.A.S.P.*, **115**, 688.
 Kelson, D. D. 2006, *Astron. J.*, , submitted.
 Mathieu, R. D. 2005, in *ASP Conf. Ser., Tidal Evolution and Oscillations in Binary Stars*, eds. A. Claret, A. Gimenez and J.-P. Zahn (San Francisco: ASP), **333**, 26.
 Muterspaugh, M. W., Lane, B. F., Konacki, M., Burke, B. F., Colavita, M. M., Kulkarni, S. R., Shao, M. 2005, *Astron. J.*, **130**, 2866.

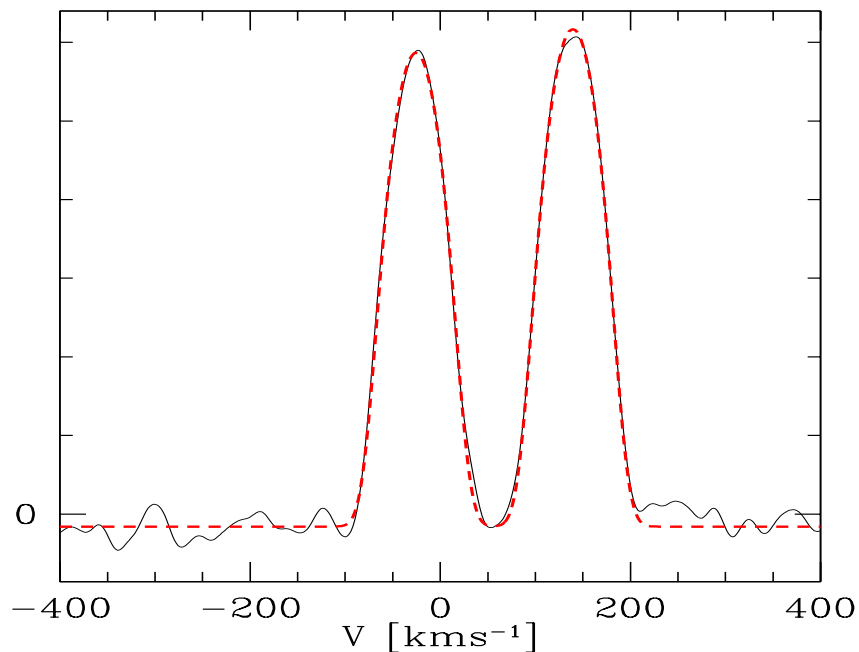


Fig. 2. Broadening Function extracted from a spectrum of NV CMa obtained at orbital phase 0.61 (solid line). The dashed line shows the fit of a model BF to the observed one.

Nordstrom, B., et al. 2004, *Astron. Astrophys.*, **419**, 989.

Plewa, T. 1988, *Acta Astron.*, **38**, 415.

Prša, A., Zwitter, T. 2005, *Astrophys. J.*, **628**, 426.

Ramírez, I., Meléndez, J. 2005, *Astrophys. J.*, **626, 465.**

Rucinski, S. M. 2002, *Astron. J.*, **124**, 1746.

VandenBerg, D. A., Clem, J. L. 2003, *Astron. J.*, **126**, 778.

VandenBerg, D. A., Bergbusch, P. A., Dowler, P. D. 2006, *Astrophys. J. Suppl. Ser.*, **162**, 375.

van Hamme, W. 1993, *Astron. J.*, **106**, 2096.

Wilson, R. W., Devinney, E. J. 1971, *Astrophys. J.*, **166**, 605.

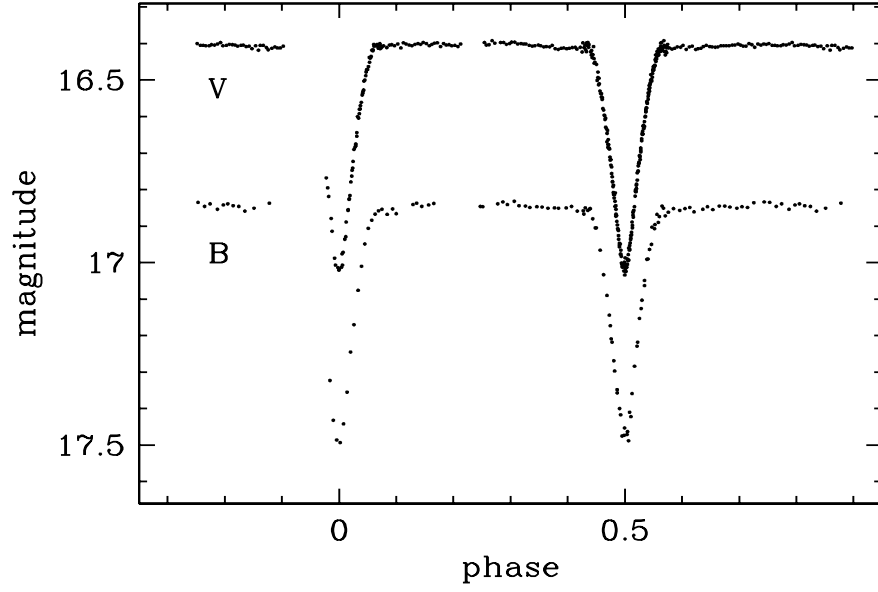


Fig. 3. Phased *BV* light curves of NV CMa.

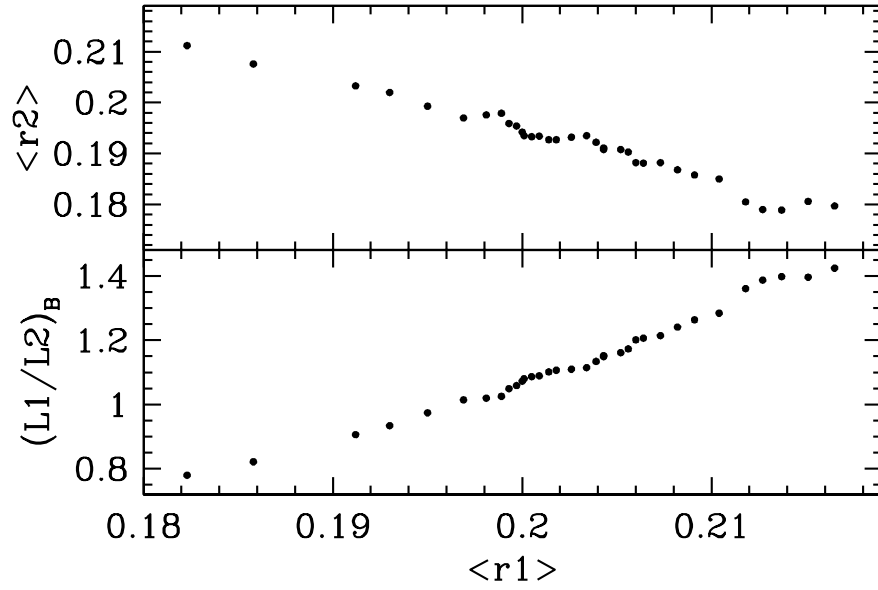


Fig. 4. Dependence of the luminosity ratio (L_{1B}/L_{2B}) and relative radius $\langle r_2 \rangle$ on the assumed radius $\langle r_1 \rangle$.

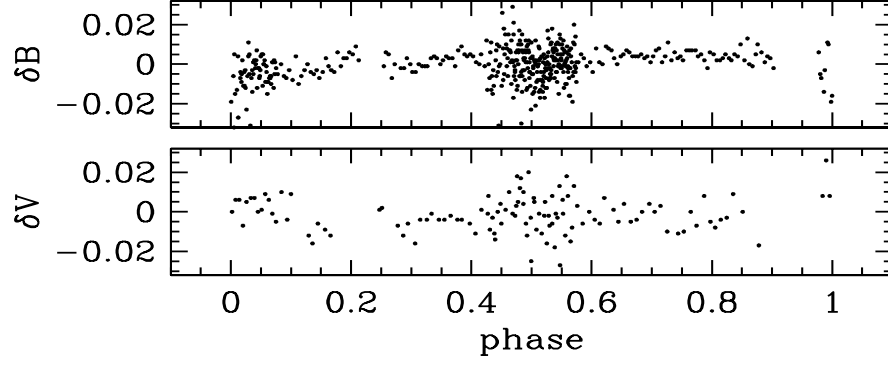


Fig. 5. The residuals for the fit corresponding to the light curve solution listed in Table 5.

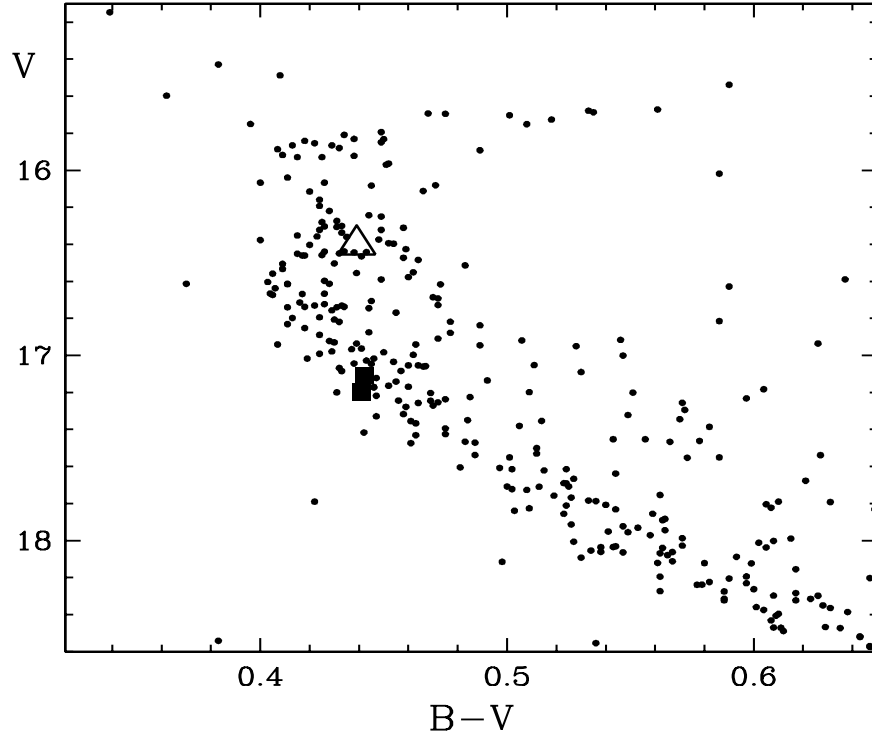


Fig. 6. Color-magnitude diagram for the turnoff region of NGC 2243. The location of NV CMA is marked with an open triangle. The squares denote the locations of individual components of the binary.

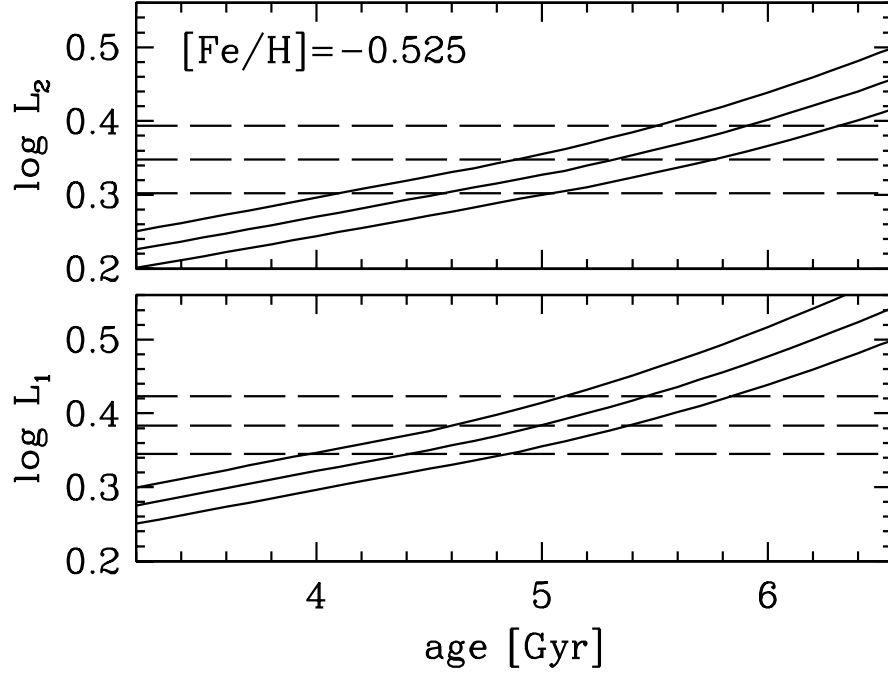


Fig. 7. Theoretical age-luminosity relations for masses $M_1 = 1.089 \pm 0.010 M_\odot$ (lower) and $M_2 = 1.069 \pm 0.010 M_\odot$ (upper). Horizontal dashed lines mark 1σ ranges for the observed luminosities of the components of NV CMa. The solid lines represent the mass $\pm 1\sigma$.

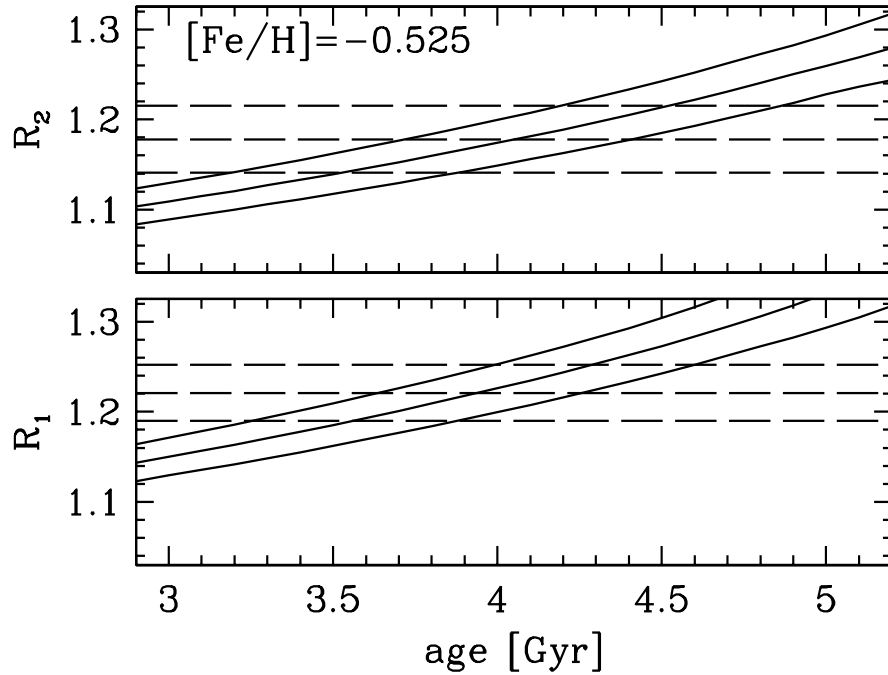


Fig. 8. Theoretical age-radius relations for masses $M_1 = 1.089 \pm 0.010 M_\odot$ (lower) and $M_2 = 1.069 \pm 0.010 M_\odot$ (upper). Horizontal dashed lines mark 1σ ranges for the observed radii of the components of NV CMa. The solid lines represent the mass $\pm 1\sigma$.

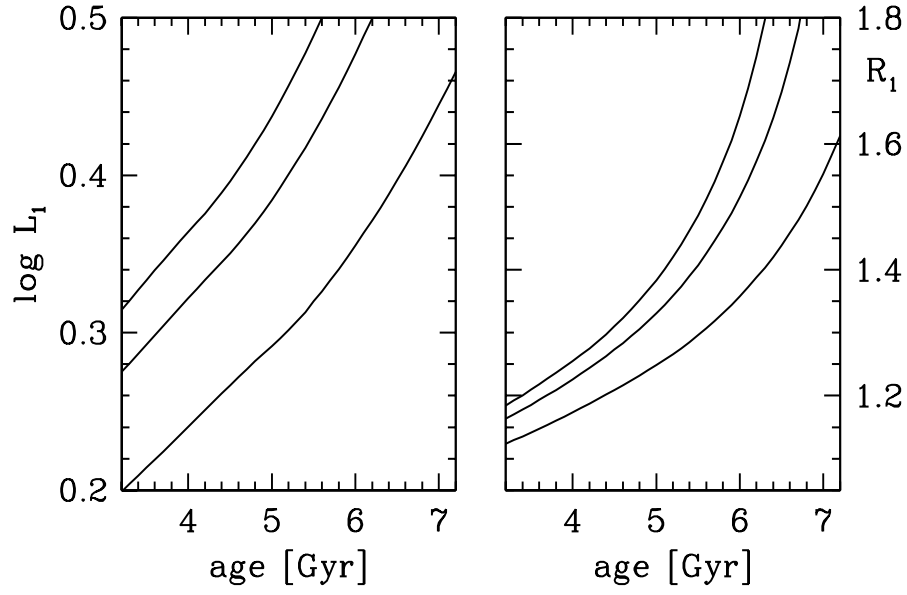


Fig. 9. Theoretical age-luminosity and age-radius relations for a star with mass $M=1.089M_{\odot}$ and for metallicity $[\text{Fe}/\text{H}]=-0.606$ (upper curve), $[\text{Fe}/\text{H}]=-0.525$ (middle curve) and $[\text{Fe}/\text{H}]=-0.397$ (lower curve).